


---

**Article:**
Edmans, J.G., Murdoch, C. orcid.org/0000-0001-9724-122X, Santocildes-Romero, M.E. et al. (3 more authors) (2020) Incorporation of lysozyme into a mucoadhesive electrospun patch for rapid protein delivery to the oral mucosa. Materials Science and Engineering: C, 112. 110917. ISSN 0928-4931

https://doi.org/10.1016/j.msec.2020.110917

---

Materials Science & Engineering C 112 (2020) 110917

Contents lists available at ScienceDirect

Materials Science & Engineering C

journal homepage: www.elsevier.com/locate/msec

# Incorporation of lysozyme into a mucoadhesive electrospun patch for rapid protein delivery to the oral mucosa

Jake G. Edmans[a,b], Craig Murdoch[a], Martin E. Santocildes-Romero[c], Paul V. Hatton[a], Helen E. Colley[a,*], Sebastian G. Spain[b]

[a] School of Clinical Dentistry, 19 Claremont Crescent, University of Sheffield, Sheffield S10 2TA, UK
[b] Department of Chemistry, Brook Hill, University of Sheffield, Sheffield S3 7HF, UK
[c] AFYX Therapeutics, Lergravsej 57, 2. tv, 2300 Copenhagen, Denmark

ARTICLE INFO

*Keywords:*
Electrospinning
Drug delivery
Proteins
Mucoadhesion
Oral medicine

ABSTRACT

The delivery of biopharmaceuticals to the oral mucosa offers a range of potential applications including antimicrobial peptides to treat resistant infections, growth factors for tissue regeneration, or as an alternative to injections for systemic delivery. Existing formulations targeting this site are typically non-specific and provide little control over dose. To address this, an electrospun dual-layer mucoadhesive patch was investigated for protein delivery to the oral mucosa. Lysozyme was used as a model antimicrobial protein and incorporated into poly(vinylpyrrolidone)/Eudragit RS100 polymer nanofibers using electrospinning from an ethanol/water mixture. The resulting fibrous membranes released the protein at a clinically desirable rate, reaching 90 ± 13% cumulative release after 2 h. Dual fluorescent fibre labelling and confocal microscopy demonstrated the homogeneity of lysozyme and polymer distribution. High encapsulation efficiency and preservation of enzyme activity were achieved (93.4 ± 7.0% and 96.1 ± 3.3% respectively). The released lysozyme inhibited the growth of the oral bacterium *Streptococcus ratti*, providing further evidence of retention of biological activity and illustrating a potential application for treating and preventing oral infections. An additional protective poly (caprolactone) backing layer was introduced to promote unidirectional delivery, without loss of enzyme activity, and the resulting dual-layer patches displayed long residence times using an in vitro test, showing that the adhesive properties were maintained. This study demonstrates that the drug delivery system has great potential for the delivery of therapeutic proteins to the oral mucosa.

## 1. Introduction

Due to advances in protein synthesis in recent decades, proteins and peptides now represent one of the fastest growing classes of pharmaceuticals [1]. The ability to modify the chemical structure of native proteins allows the development of more stable analogues with high specificity, high potency, and low toxicity, resulting in higher success rates than traditional small molecule new chemical entities in clinical development stages [2]. A variety of potential applications for biopharmaceutical delivery to the oral mucosa have been identified. These include antimicrobial peptides as a treatment for bacterial [3] and fungal [4] infections, such as in periodontal disease or oral candidiasis, with resistance to traditional antimicrobials. Topical recombinant cytokines such as epidermal growth factor and basic fibroblast growth factor have shown potential in vivo for regenerating oral wounds or ulcers caused by oral mucositis [5,6]. Some therapeutic peptides, including salmon calcitonin and insulin, in combination with permeation enhancers, have been shown in animals or humans to permeate the oral mucosa sufficiently to achieve therapeutic doses [7,8]. Therefore, the oral mucosa is also of interest for systemic delivery, circumventing proteolytic degradation in the gastrointestinal tract and offering the potential for controlled release and needleless delivery.

A significant challenge for the delivery of proteins to the oral mucosa is the lack of suitable formulations that allow specific delivery. The most commonly used formulations targeting the oral mucosa include mouthwashes [9], gels [10], tablets [11], and dissolvable films [12]. These drug delivery systems work well for highly permeable drugs [13] but release of the active ingredient is often non-specific, across the entire oral cavity rather than localised into a specific region of the oral mucosa where the drug is required. Variations in salivary flow and mechanical forces mean that doses are poorly defined where prolonged contact is required. To address this, we have developed an electrospun

* Corresponding author.
*E-mail address:* h.colley@sheffield.ac.uk (H.E. Colley).

https://doi.org/10.1016/j.msec.2020.110917
Received 7 January 2020; Received in revised form 4 March 2020; Accepted 31 March 2020
Available online 01 April 2020

mucoadhesive patch with a backing layer film to promote unidirectional drug delivery [14]. The system is comprised of FDA-approved polymers and offers several advantages over existing alternatives including in vivo residence times of up to 2 h, high patient acceptability, high surface area, and fast release rates [15]. This system in currently undergoing phase 2 clinical trials for the delivery clobesasol-17-propionate to treat oral lichen planus. The patches also show early promise for the delivery of lidocaine as a topical dental anaesthetic or analgesic [16].

A range of proteins and peptides have previously been encapsulated into polymer nanofibers using electrospinning [17]. However, most examples of electrospun drug delivery systems focus on biodegradable polyesters, which tend to require chlorinated solvents to achieve solubility. This leads to concerns over protein denaturation and loss of activity [17]. Several different approaches for incorporating proteins into electrospun membranes have been identified, for example, surface functionalisation by chemically bonding proteins to pre-spun fibres [18]. However, this immobilises the protein and is therefore more relevant for slow release applications. Much current work focuses on electrospinning emulsions or suspensions to allow electrospinning of proteins and polymers with incompatible solvent requirements [19,20]. This can result in activity loss and poor encapsulation efficiency due to the solvent phases having different conductivities and separating during the spinning process. Two separate solutions may also be electrospun into core-shell fibres using coaxial electrospinning with two capillary feeding channels [21]. Proteins encapsulated in the fibre core from aqueous solutions have been shown to maintain some or all of their activity [22,23]. However, the outer sheath layer is likely to influence drug release profiles and the manufacturing process is considerably more complex. To date, there are no published studies describing the encapsulation and release of bioactive proteins from a single-phase organic solvent mixture using uniaxial electrospinning. Here, we report the incorporation of lysozyme as a model protein into an electrospun mucoadhesive patch and investigate its potential for therapeutic protein delivery. This protein delivery system is unique in that it uses a simple uniaxial electrospinning manufacturing process to encapsulate a biologically active protein into an insoluble drug delivery system. For the first time, we show that proteins encapsulated in these uniaxial fibres retain biological activity upon release and significantly advance the field of electrospun-mediated protein delivery.

## 2. Methods

### 2.1. Materials

Poly(vinylpyrrolidone) (PVP; $M_W$ 2000 kDa) and Eudragit RS100 (RS100; $M_W$ 38 kDa) were kindly donated by BASF, UK and Evonik Industries AG, Germany, respectively. Poly(caprolactone) (PCL; $M_W$ 80 kDa), dichloromethane (DCM), lysozyme from chicken egg white, lyophilised *Micrococcus lysodeikticus* cells, phosphate-buffered saline tablets, fluorescein isothiocyanate isomer I (FITC), Texas red sulfonyl chloride, sodium bicarbonate, and sodium carbonate were purchased from Sigma-Aldrich (Poole, UK). Ethanol and dimethylformamide (DMF) were purchased from Fischer Scientific (Loughborough, UK). Pierce™ BCA protein assay kit was purchased from Thermo Scientific (Loughborough, UK). Brain heart infusion broth was purchased from Oxoid (Basingstoke, UK).

### 2.2. Electrospinning system

Electrospun membranes were fabricated using a system composed of a PHD2000 syringe pump (Havard Apparatus, Cambridge, UK) and an Alpha IV Brandenburg power source (Brandenburg, Worthing, UK). Plastic syringes (1 mL volume; Henke Sass Wolf, Tuttlingen, Germany) were used to drive the solutions into a 20-gauge blunt metallic needle (Fisnar Europe, Glasgow, UK). Electrospinning was performed at room temperature with a potential difference of 19 kV, a flow rate of 2 mL/h, and a flight path of 14 cm.

### 2.3. Preparation of polymer solutions and fabrication of bioadhesive membranes

All electrospinning solutions contained 0.1025 ± 0.00025 g/mL PVP and 0.1225 ± 0.0005 g/mL Eudragit RS100 (by total solvent volume before mixing). The required amounts of PVP and RS100 were added to ethanol or an ethanol/water mixture and mixed at room temperature using a magnetic stirrer until dissolved. Lysozyme was dissolved in ice cold PBS (75 mg/mL) and added to the polymer solution and stirred until uniformly distributed, contributing 3 v/v % to the final solvent composition. Electrospinning was started within 1 min of adding the lysozyme. Placebo solutions and membranes were prepared using 3 v/v % distilled water instead of lysozyme in PBS.

### 2.4. Conductivity of polymer solutions

Electrical conductivity of the polymeric solutions was measured using a Mettler Toledo FG3 conductivity meter (Mettler Toledo, Schwerzenbach, Switzerland), applying a conductivity standard of 1413 μS $cm^{-1}$ (Mettler Toledo).

### 2.5. Rheology of polymer solutions

The viscosity of the polymeric solutions was measured using an MCR 301 rheometer (Anton Paar, Graz, Austria) with a cone-plate measuring system CP25-4/IMG1 (25 mm diameter, 4° cone angle, and 253 μm truncation) at a constant temperature (25 ± 0.1 °C) and a sample volume of approximately 0.4 mL. Logarithmic shear rate sweep tests were performed with 31 points in the range of 0.1 to 100 $s^{-1}$ lasting 20 s per point.

### 2.6. Scanning electron microscopy

Electrospun membranes were imaged using a TESCAN Vega3 scanning electron microscope (SEM; Tescan, Cambridge, UK). Samples were sputter coated with gold and imaged using an emission current of 10 kV. All images were processed using ImageJ software tools [24]. Fibre diameters were measured by ImageJ, using randomly generated coordinates and a superimposed grid to select fibres to measure. Three images were analysed for each composition with at least 10 measurements per image.

### 2.7. Degree of swelling of electrospun membranes

Pre-weighed 15 mm discs (5–14 mg) were placed in sample tubes with 1 mL distilled water for 2 h. If intact, samples were removed, and each side pressed against a glass surface to remove excess water before reweighing. The percentage degree of swelling was calculated using the formula:

$$\frac{(M_s - M_d)}{M_d} \times 100$$

where $M_s$ is the mass of the sample after swelling in distilled water and $M_d$ is the dry mass of the sample before swelling.

### 2.8. Activity and encapsulation efficiency measurement

Electrospun membrane (9–12 mg) was prepared and immersed in 2 mL PBS for 24 h. to elute the protein. A bicinchoninic acid (BCA) protein assay was used as directed to determine encapsulation efficiencies. Absorbance was measured at 562 nm using a spectrophotometer (Tecan, Theale, UK). The apparent mass fraction determined from the protein concentrations in the samples was

normalised against the dry mass fraction of lysozyme in the electrospinning solution.

Lysozyme enzyme activity in samples was measured using a photometric enzyme kinetic assay as previously described [25]. Briefly, 10 μL of membrane supernatant diluted in PBS (1:10, v/v) was added to a clear plastic 96-well plate along with 200 μL of lyophilised *Micrococcus lysodeikticus* cells (0.4 mg/mL in PBS). The change in optical density at 450 nm ($OD_{450}$) was measured over time for 10 min. Active lysozyme concentrations of the samples were interpolated from a standard curve created using lysozyme standards (0, 20, 40, 60, 80, and 100 μg/mL) and normalised against the total protein concentration.

### 2.9. Homogeneity of lysozyme incorporation

Electrospun membranes were divided into three concentric regions: the central circle of the membrane with one third the diameter of the whole membrane, an intermediate ring with two thirds the diameter of the whole membrane, and the remaining outer ring. The activity and encapsulation efficiencies of the different regions where measured as previously described.

### 2.10. Fluorescent labelling of PVP and lysozyme

To label PVP, a complex with fluorescein isothiocyanate isomer I (FITC), as described by Aulton et al., was produced [26]. FITC in 0.1 M pH 9.2 carbonate-bicarbonate buffer (2 mg/mL, 1 mL) was added dropwise with vigorous stirring to PVP in the same buffer (25 mg/mL, 10 mL) in an opaque sample tube. The tube was sealed and incubated at room temperature for 3 h. The complex was purified by adding dropwise with stirring to acetone (500 mL) and the precipitate collected and washed with acetone (2 × 10 mL). Excess solvents were removed by freeze drying.

Lysozyme was labelled with Texas red sulfonyl chloride. Texas red sulfonyl chloride (1 mg) was added, with vigorous stirring until dissolved, to lysozyme in 0.1 M pH 9.2 carbonate-bicarbonate buffer (75 mg/mL, 1 mL) in an opaque sample tube. The tube was sealed and incubated at room temperature for 24 h and the product purified using gel permeation chromatography with Sephadex G-25 and PBS. The solvent was removed by freeze drying.

### 2.11. Fabrication and imaging of fluorescent electrospun fibres

Electrospun fibres were prepared as previously described with 97 v/v % ethanol but using Texas red labelled lysozyme and substituting 24 w/v % of the PVP with the FITC-PVP complex where appropriate. Samples were placed on glass slides and overlaid with glass cover slips. Imaging was performed in dual-channel mode using a Nikon A1 laser scanning confocal microscope with 457–514 nm argon and 561 nm sapphire lasers. All images were processed using ImageJ software tools [24].

### 2.12. Release profile

Samples of electrospun membranes (20 mg) were immersed in 4 mL PBS and 10 μL samples taken at time intervals (0, 10, 20, 30, 60, 120, 180 min.) following vortexing for 5 s. Active lysozyme concentration was measured as previously described. To calculate cumulative release, the active concentration was normalised against the theoretical maximum concentration, assuming 100% encapsulation efficiency, release, and activity.

### 2.13. Growth inhibition assay with Streptococcus ratti

*Streptococcus ratti* (NCTC 10920, Public Health England, Salisbury, UK) was grown overnight in 10 mL brain heart infusion broth (BHI) at 37 °C, 5% $CO_2$ before diluting to $OD_{600}$ of 0.1 in BHI. Samples of electrospun membrane (50 ± 0.1 mg) were immersed in 1 mL sterile PBS for 24 h with vortexing for 30 s after immersing and before sampling the eluate. Sterile PBS was used as a negative control and 0.5 mg/mL lysozyme in PBS as a positive control. Additionally, placebo patch samples were eluted in a stock 0.5 mg/mL lysozyme solution. A 12-well plate was filled with BHI (0.5 mL per well) before adding eluate and controls in triplicate (0.5 mL). Each well was inoculated with 0.1 mL bacteria and the plate incubated at 37 °C with $OD_{600}$ measured every 10 min for 15 h with shaking for 1 min before each reading.

### 2.14. Fabrication of hydrophobic backing layer

The hydrophobic backing layer (BL) was prepared by electrospinning a PCL solution on top of the bioadhesive PVP/RS100 layer. PCL was added to a blend of DCM and DMF (90:10 v/v %) and stirred at room temperature until dissolved to prepare a solution of concentration 10 w/v %. To enhance the attachment between the bioadhesive and backing layer a thermal treatment was applied by heating at 65 °C for 15 min in a dry oven.

### 2.15. In vitro adhesion study of dual-layer patches

The adhesive properties of electrospun membranes with backing layers were investigated in vitro. For each composition, two discs of 1 cm diameter were cut from three membranes (n = 6) and applied to 20 μL droplets of PBS on a plastic petri dish with gentle pressure from the index finger for 5 s. The petri dishes were filled with PBS (20 mL) and then incubated on an orbital shaker at 250 rpm at room temperature for a total of 2 weeks. The samples were inspected daily to observe any detachment of the backing layer.

### 2.16. Data analysis

All data and statistical analyses were performed using GraphPad Prism 8.0 software (GraphPad Software, La Jolla, CA). One-way ANOVA with post hoc Tukey tests or Welch's *t*-tests were used to compare differences between groups and results considered statistically significant if $p < 0.05$.

## 3. Results and discussion

### 3.1. Physical properties of solutions

The morphology of electrospun fibres is strongly influenced by processing parameters and solution properties. Conductivity and viscosity measurements were used to determine how the addition of a protein affects solution properties. A typical dose of a therapeutic peptide is in the order of micrograms [27–29], therefore a loading of 1% lysozyme by dry mass was used to simulate a loading that may be suitable for mucosal peptide or protein delivery. Including lysozyme in PBS caused an increase in solution conductivity from 118.4 ± 7.2 to 168.6 ± 8.6 μS/cm ($p = 0.0247$) and an increase in viscosity at 5 $s^{-1}$ from 1.14 ± 0.18 to 1.477 ± 0.091 Pa·s ($p = 0.0369$) in comparison to the equivalent solution prepared with distilled water. The increase in conductivity on addition of lysozyme, a cationic protein, was expected due to increased electrolyte concentration. The increase in viscosity is typical of a protein solution [30]. An organic solvent such as ethanol is required for the dissolution of RS100, however ethanol can act as a protein denaturant [31]. It was therefore hypothesised that reducing the proportion of ethanol in the electrospinning solvent mixture would improve protein activity. Therefore, solvent mixtures with different proportions of ethanol were investigated. Decreasing the proportion of ethanol in the solution and replacing with water caused a linear increase in conductivity ($R^2 = 0.9878$) reaching 504 ± 33 μS/cm at 40 v/v % ethanol (Fig. 1A). This follows a similar trend to that previously reported for pure ethanol-water mixtures and is expected due to ethanol

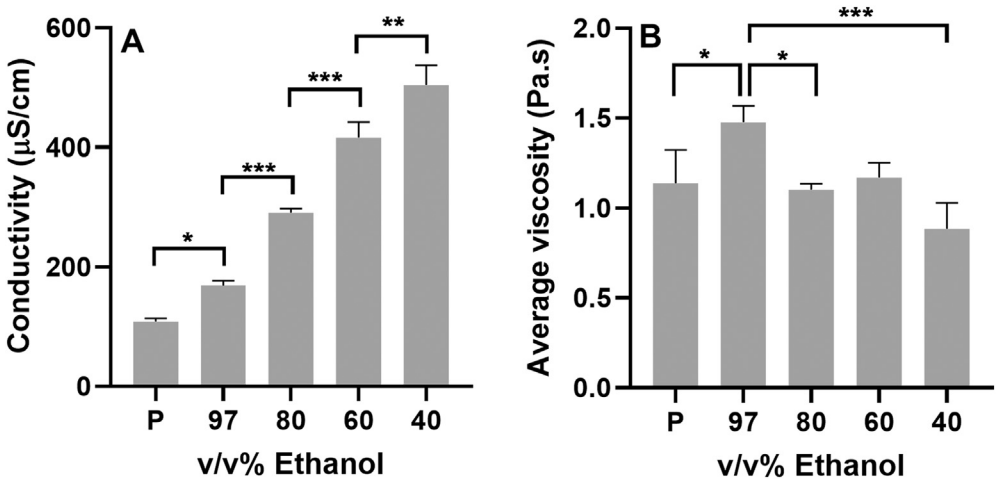


**Fig. 1.** Conductivity of electrospinning solutions containing lysozyme with different mixtures of ethanol and water as solvents and placebo (P) solutions in 97 v/v % ethanol without lysozyme (A). Viscosity of electrospinning solutions measured at a shear rate of 5 $s^{-1}$ (B). Data are presented as mean ± SD, with 3 independent repeats and analysed using one-way ANOVA with post hoc Tukey tests. *, $p < 0.05$; **, $p < 0.01$; ***, $p < 0.001$.

having a much lower conductivity than water [32]. Reducing the proportion of ethanol from 97 to 80 v/v % reduced viscosity from 1.477 ± 0.091 to 1.103 ± 0.032 Pa·s ($p = 0.0214$, Fig. 1B). The decrease in viscosity at lower ethanol concentrations is consistent with polymers adopting a globule conformation with a smaller hydrodynamic volume due to poorer solvation. PVP in ethanol-water mixtures has previously been shown to have a reduced hydrodynamic radius at lower ethanol concentrations, suggesting a transition from chains to less solvated globules [33]. RS100 is a less hydrophilic, water-insoluble polymer, therefore it is also likely to be poorly solvated at lower ethanol concentrations. All polymer solutions behaved approximately as Newtonian fluids with no clear shear thickening or thinning trend (Fig. S1).

### 3.2. Fabrication and morphology of electrospun membranes

Electrospun fibres containing 1 w/v % lysozyme and made using 97, 80, 60, and 40 v/v % ethanol mixed with distilled water as solvent and a placebo membrane manufactured with 97 v/v % ethanol without lysozyme were analysed by scanning electron microscopy. All samples had some merged fibres and almost no bead defects (Fig. 2). No other defects were observed. Including lysozyme caused a decrease in diameter from 2.50 ± 0.71 to 2.04 ± 0.92 µm ($p = 0.0402$). The reduced fibre diameter is consistent with the observed increase in conductivity, which allows the polymer solution to hold more charge, resulting in more efficient elongation in the electric field. There was no significant difference in diameter between 97 and 80 v/v % ethanol, however there was a significant decrease in fibre diameter from 2.34 ± 0.63 µm to 1.28 ± 0.41 µm ($p < 0.0001$) and 0.58 ± 0.13 µm ($p < 0.0001$) when the ethanol content was reduced from 80 v/v % to 60 and 40 v/v % ethanol respectively. Higher solution conductivity and lower viscosity are well known to be associated with narrower fibres [34], therefore these measurements broadly follow the trend expected from the solutions properties. These results also similar to those reported by Nartetamrongsutt et al., who showed that including ionic salts in solutions of PVP in ethanol-water mixtures resulted in reduced fibre diameters and increased solution conductivity [35]. They also found that reducing the proportion of ethanol below 50 v/v % resulted in narrower fibres and a narrower distribution of fibre diameters along with reduced solution viscosity and increased solution conductivity.

### 3.3. Swelling and integrity of electrospun membranes

To be suitable as a mucoadhesive drug delivery system, the protein-loaded membranes must swell to promote adhesion but also remain intact in a wet environment. Samples were placed in distilled water for 2 h and visually inspected for loss of integrity and, where possible, the degree of swelling was measured. All samples electrospun using 40 v/v % ethanol and one of three membranes using 60 v/v % ethanol rapidly disintegrated into small insoluble particles when added to water. In contrast, fibres electrospun from 97 and 80 v/v % ethanol and placebo membranes remained intact after 2 h and did not differ significantly in degree of swelling (Fig. 3, $p = 0.4342$). These data suggest that 97 or 80 v/v % ethanol are suitable solvents for this polymer system and application. The disintegration of narrower fibres may be a result of PVP-rich domains rapidly dissolving and creating discontinuations in the fibres. This would be expected of narrower fibres, since the smaller diameter would make it easier for discontinuations to form and the higher surface area and smaller contacts between fibres facilitates the rapid dissolution of PVP.

### 3.4. Effect of solvent mixture on encapsulation and activity

Lysozyme was eluted from the fibres and the amount released measured using a protein assay and its activity assessed using an enzyme kinetic assay relative to freshly prepared lysozyme stock solutions. Encapsulation efficiency ranged from 75 ± 10 to 98 ± 8%, and no statistically significant difference between solvents was shown (Fig. 4, $p = 0.0750$). It was initially hypothesised that reducing the concentration of ethanol in the electrospinning solution would limit protein denaturation, leading to higher enzyme activity. However, it was found that enzyme activity was close to 100% (96 ± 3 to 108 ± 18%) with no difference between the solvent mixtures tested. Placebo membranes were used as negative controls and showed apparent protein loading, as measured by a BCA assay, close to zero, 0.017 ± 0.015 w/w % compared to 0.928 ± 0.070 w/w % for lysozyme loaded membranes ($p < 0.005$). The activity of the placebo patches was also close to zero, corresponding to an active lysozyme loading of 0.055 ± 0.042 w/w % compared to 0.892 ± 0.049 w/w % for lysozyme-loaded membranes ($p < 0.0005$). This shows that the observed protein release and enzyme activity was not a false positive caused by dissolved polymer. Changing the ratio of solvents did not provide a noticeable benefit in terms of activity, therefore further experiments focused on 97 v/v % ethanol as the solvent, which gave an encapsulation efficiency of 93 ± 7% and activity of 96 ± 3%. The high encapsulation efficiencies reported here are comparable to those previously reported for small molecule drugs encapsulated using uniaxial electrospinning. For example, Xie et al., reported the encapsulation of paclitaxel in PLGA nanofibers with loading of around 10 w/w % and an encapsulation efficiency over 90% [36]. There is very little published research reporting encapsulation of active proteins using uniaxial electrospinning of a single phase solution. Eriksen et al., incorporated a fluorescently-labelled antimicrobial peptide into PCL

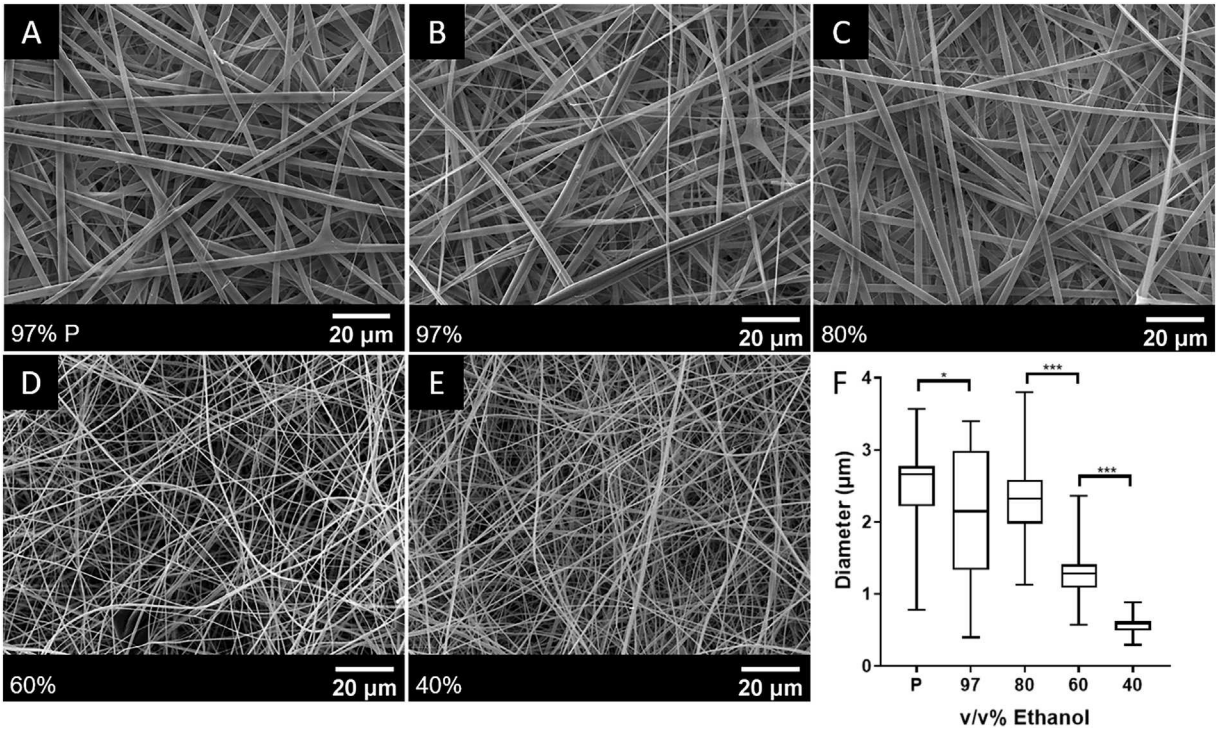


**Fig. 2.** Scanning electron micrographs of a placebo membrane (A) and electrospun fibres containing lysozyme manufactured using different concentrations of ethanol, shown in bottom left as v/v% (B–E). Fibre diameter distributions (F). Data are presented as median, interquartile range, and range with 3 independently prepared samples for each solvent mixture and 10 diameter measurements per sample and analysed using one-way ANOVA with post hoc Tukey tests. *, $p < 0.05$; ***, $p < 0.001$.

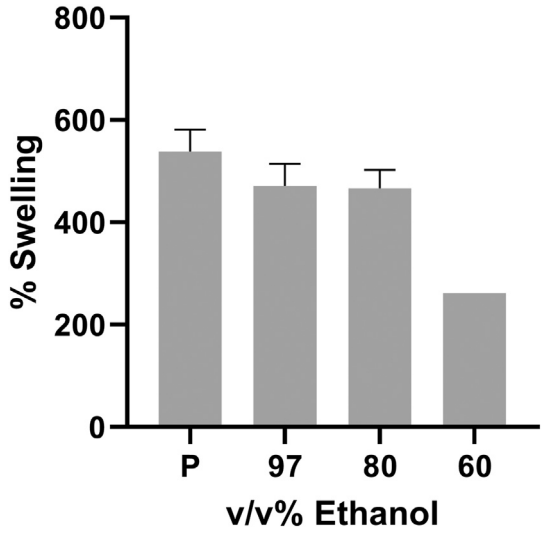


**Fig. 3.** Degree of swelling in water of lysozyme-containing electrospun fibres using different ethanol concentrations and placebo membranes (P). Data are presented as mean ± SD, with 3 independent samples and analysed using one-way ANOVA with post hoc Tukey tests. For 60 v/v % ethanol only 2 independent measurements could be made, therefore SD was not calculated.

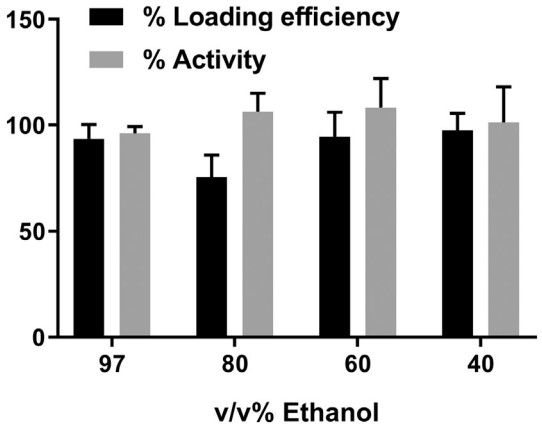


**Fig. 4.** Encapsulation efficiency and activity of lysozyme in fibres electrospun using different mixtures of ethanol and water as solvents. Data is presented as mean ± SD, with 3 independent samples per solvent mixture, and analysed using one-way ANOVA with post hoc Tukey tests.

fibres at a loading of approximately 0.1 w/w% using a miscible methanol/chloroform solvent mixture, but were unable to confirm biological activity [37]. Conversely, emulsion and coaxial electrospinning, with the protein in an aqueous phase, have been frequently studied for protein encapsulation. Due to separation of solvent phases in the Taylor cone, emulsion electrospinning often results in low encapsulation efficiencies of only a few percent for globular proteins [19], however a higher efficiency of 87.2 ± 1.8% has been achieved for collagen-like protein in poly(lactic-*co*-glycolic acid) (PLGA) fibres at a loading of 5 w/w% [20]. Ji et al., compared emulsion and coaxial electrospinning for the encapsulation of alkaline phosphatase into PCL fibres at a loading of 0.16 w/w% from water and 2,2,2-trifluoroethanol [23]. Coaxial electrospinning resulted in 76.2 ± 8.4% enzyme activity, while electrospinning from an emulsion resulted in 49.3 ± 4.5% activity. Lysozyme has also previously been encapsulated in PCL/poly (ethylene glycol) (PEG) fibres using coaxial electrospinning at loadings of 2–6 w/w% and shown to be active, however the activity was not quantified [22]. The polymer/solvent system described here enables encapsulation efficiencies and activity preservation superior to what has been achieved previously with uniaxial single phase and emulsion electrospinning and at least as high as that achieved with coaxial electrospinning.

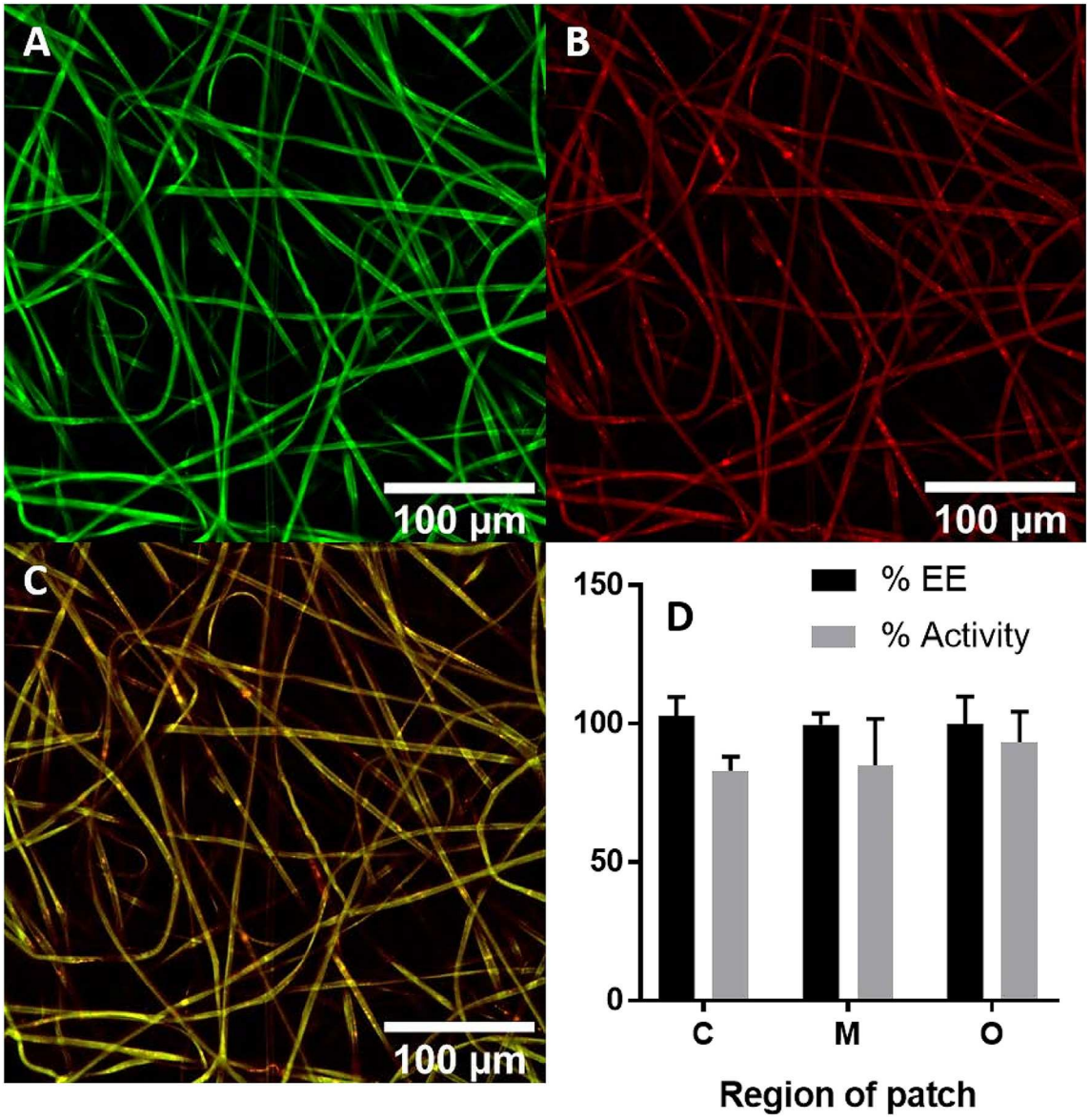


**Fig. 5.** Confocal micrographs of electrospun fibres containing FITC-PVP complex and Texas-red conjugated lysozyme to show the distribution of PVP (A, green) and lysozyme (B, red) within the fibres and an overlay of both distributions (C). Encapsulation efficiency (EE) and activity of central, intermediate, and outer regions of lysozyme-containing membranes electrospun from 97 v/v % ethanol (D). Data is presented as mean ± SD, with 3 independent samples for each region, and analysed using one-way ANOVA with post hoc Tukey tests. (For interpretation of the references to color in this figure legend, the reader is referred to the web version of this article.)

### 3.5. Homogeneity of electrospun membranes

To determine the distribution of PVP and lysozyme within the fibres a novel dual fluorescent labelling approach was used. A FITC-PVP complex and Texas red conjugated lysozyme were added before electrospinning and the resulting fibres imaged using confocal microscopy. Singly labelled control samples showed that signals were not caused by auto fluorescence or crosstalk between channels (Fig. S2). PVP appears to be homogenously distributed within the fibres, with any polymer phase separation occurring over a nanometre scale below the resolution of the microscope (Fig. 5A). Lysozyme is fully incorporated into the fibres and almost homogeneously distributed (Fig. 5B). Some aggregation is viably present over a microscopic scale as bright regions, however this does not appear to significantly affect its activity. To determine the homogeneity of the lysozyme distribution over a macroscopic scale, the loading and activity of different regions (centre, intermediate, outer edge) of the membrane were compared (Fig. 5D). The loading and activity were similar across all regions tested indicating that the protein is homogeneously distributed at the macroscopic level.

### 3.6. Characterisation of release kinetics using an enzymatic assay

We previously showed that a mucoadhesive drug delivery device with a similar polymer composition had a residence time of 96 ± 26 min when applied to the human buccal oral mucosa [15]. To be useful as a mucosal peptide delivery system, the membranes must release their payload over a similar timescale. To measure the release profile, lysozyme was eluted from the fibres and the active concentration measured using enzyme kinetics for up to 3 h (Fig. 6). Lysozyme was released rapidly with 76 ± 23% released within 30 min and 88 ± 16% within 1 h. The release then begins to plateau, reaching 90 ± 13% after 2 h. The release is likely to be facilitated by rapid water penetration due to the dissolution of PVP and the swelling of

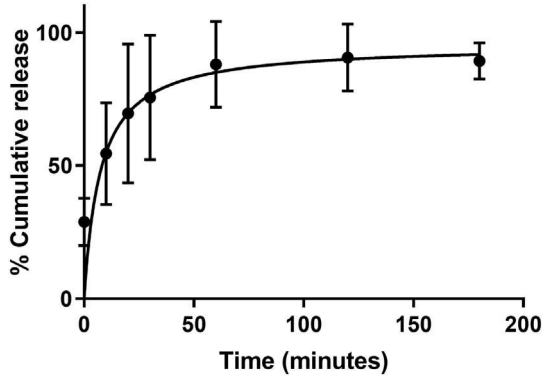


**Fig. 6.** Cumulative release of lysozyme from membranes electrospun using 97 v/v % ethanol as a solvent following immersion in PBS. Data is presented as mean ± SD, with 3 independent samples for each time point.

RS100. The lack of sheath layer associated with coaxial electrospinning also increases release rate by decreasing the diffusion path required for release [38]. Proteins previously encapsulated in water-insoluble polymer fibres have shown considerably slower release rates. Eriksen et al., reported that an antimicrobial peptide was released linearly from uniaxial PCL fibres, with < 50% released within 2 h [37]. Ji et al., reported that bovine serum albumin undergoes biphasic release from PCL fibres prepared both with emulsion and coaxial electrospinning, with an initial burst of around 15% released within 4 h, followed by prolonged release which begins to plateau at around 50–70% after 35 days [23]. Wei et al., showed that collagen-like protein was released from PLGA fibres prepared by emulsion electrospinning linearly for the first 1–2 weeks, reaching 50–70% depending on fibre diameter [20]. Although other polymer systems may be more suitable for sustained release over a period of days, the system reported here is unique in that it enables protein release over timescales relevant for delivery to the oral mucosa without rapidly dissolving.

### 3.7. Fabrication of backing layer and effect on activity

A film of hydrophobic PCL was introduced to act as a backing layer to promote unidirectional delivery and protect against mechanical forces in the mouth as previously described by Colley et al., in dual-layer patches for the unidirectional delivery of clobetasol to the oral mucosa [14]. PCL was electrospun on top of the protein-loaded mucoadhesive layer and the dual-layer patch heated at 65 °C to melt the PCL fibres into a continuous film. SEM micrographs show the fabrication of patches with a continuous backing film and that the fibrous structure of the lower layer was preserved (Fig. 7A–B). Activity measurements revealed that thermal treatment did not cause significant loss of enzyme activity ($p = 0.8326$). Applying dry heat at 100 °C for 1 week resulted in a decrease in activity from 84 ± 4% to 30 ± 16% ($p = 0.0017$), showing that lysozyme in the electrospun fibres is susceptible to heat denaturation in extreme conditions.

### 3.8. In vitro testing of residence time

A simple in vitro residence time test was applied to assess whether lysozyme had a detrimental effect on patch adhesion or structural integrity. Samples were applied to a petri dish, immersed in PBS and shaken for two weeks with daily inspection for detachment of the backing layer. Both the lysozyme-containing patches and the placebo patches remained attached until the end of the experiment, suggesting that lysozyme does not disrupt membrane integrity, adhesion, or attachment of the backing layer.

### 3.9. Lysozyme released from membranes inhibits the growth of *Streptococcus ratti*

Over 600 different species of microbes reside commensally within the oral cavity in healthy individuals [39]. Many of these organisms have the ability to become pathogenic if the oral mucosa is wounded or compromised, or if there is significant dysbiosis in the microbial flora. Lysozyme is a glycoside hydrolase and acts as an antimicrobial agent by catalysing the hydrolysis of linkages between *N*-acetylmuramic acid and *N*-acetyl-D-glucosamine residues in peptidoglycan, the major cell wall component of Gram-positive bacteria. We next tested if membrane-released lysozyme was able to cleave peptidoglycan and cause bacterial cell lysis in *Streptococcus ratti*, a Gram-positive oral bacterium found in the oral cavity that has been associated with dental biofilms [40] and is known to be affected by lysozyme activity [41]. Lysozyme was eluted from electrospun membranes and its effects on inhibiting bacteria growth assessed. Eluted lysozyme significantly inhibited the growth of *S. ratti* by 51% after 15 h compared to eluate from a placebo membrane control (51.1 ± 5.7 vs 0.6 ± 1.6, $p < 0.0001$, Fig. 8). These data clearly show that lysozyme released by electrospun membranes retains its biological activity and is able to inhibit bacterial growth and indicate that these membranes may be effective at treating oral bacterial infections or as covering for oral wounds or lesions that may be susceptible to bacterial infection.

Interestingly, the lysozyme membrane eluate contained 0.43 ± 0.07 mg/mL protein content and caused 51% bacterial inhibition, whereas purified lysozyme of a similar protein concentration (0.5 mg/mL) almost completely abolished *S. ratti* growth over the same time period ($p < 0.0001$, Fig. 8). To investigate the cause of this apparent reduction in activity, samples of placebo membranes were eluted in 0.5 mg/mL lysozyme solution. The resulting eluate inhibited growth

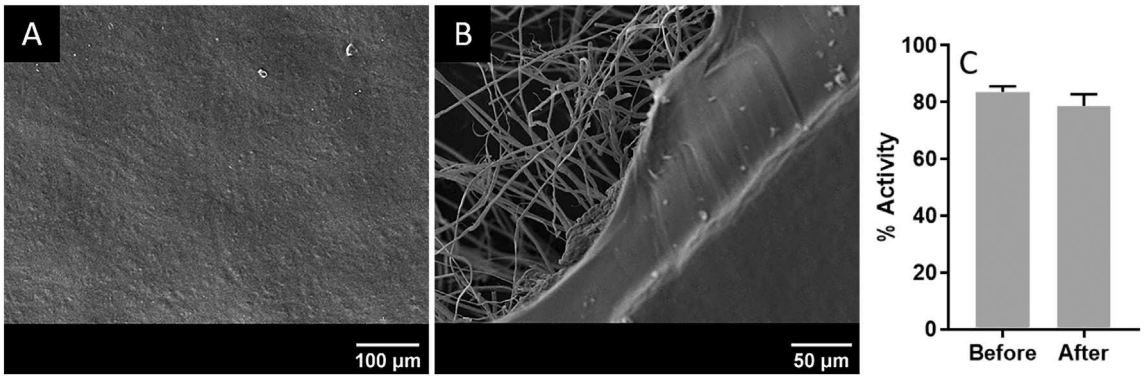


**Fig. 7.** SEM micrographs of the continuous PCL backing layer film formed after thermal treatment (A) and the edge of the patch showing the PCL film backing layer and lower layer of lysozyme-containing PVP and RS100 fibres (B). Activity of lysozyme released from patches with PCL backing layers before and after melting at 65 °C for 15 min (C). Data is presented as mean ± SD, with 3 independent samples, and analysed using Welch's *t*-test.

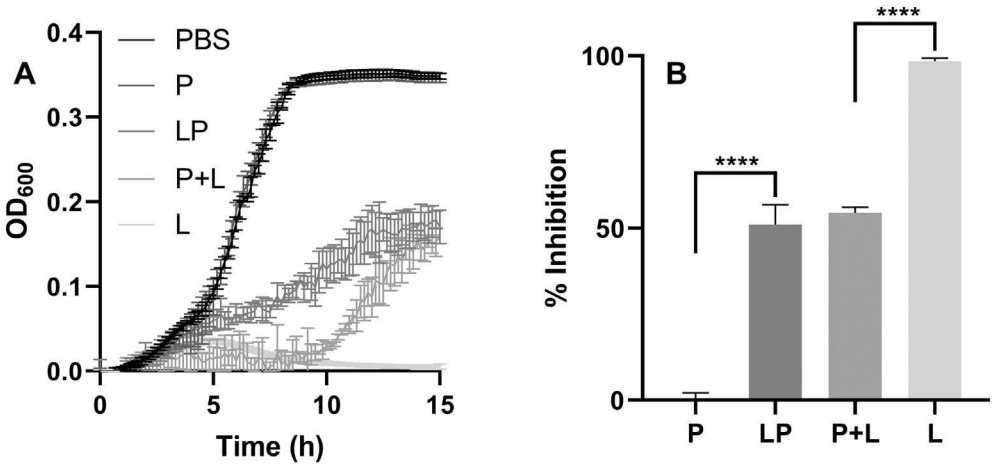


**Fig. 8.** Growth curve of *S. ratti* measured by optical density at 600 nm over time in the presence of PBS, eluent from placebo membranes (P), eluent from membranes containing lysozyme (LP), placebo membranes eluted in stock lysozyme solution (P + L), and a lysozyme stock solution (L) (A). % growth inhibition relative to PBS at 15 h (B). Data is presented as mean ± SD, with 3 independent samples, and the optical densities at 15 h analysed using one-way ANOVA with post hoc Tukey tests. ****, $p < 0.0001$.

to the same extent as the lysozyme membrane eluent, suggesting that this disparity related to polymer in the sample and not loss of activity during electrospinning. This may be a result of water soluble PVP leaching from the fibres and inhibiting lysozyme activity or encapsulating and protecting the bacteria. PVP has previously been shown to inhibit the enzyme phenolase [42], however its effect on lysozyme has not been studied. Further investigation would be required to elucidate the mechanism of this effect.

## 4. Conclusions

This mucoadhesive system enabled the encapsulation of an enzyme into polymer fibres with superior encapsulation efficiency and biological activity preservation compared to what has previously been accomplished with uniaxial electrospinning. The approach described here is considerably simpler to scale up to an industrial manufacturing setting than the frequently reported emulsion and coaxial electrospinning techniques, with fewer parameter to optimise and control. Unlike previous systems, the fibres released the majority of the protein in a single burst at a rate appropriate for drug delivery to the oral mucosa. Furthermore, the protein was homogenously distributed, and data suggest that the dual-layer patches maintained mucoadhesive properties similar to those previously reported [14]. The biological activity of the encapsulated protein was further demonstrated by the inhibition of growth of an oral bacterial strain. This illustrates that the patches could be useful for the local delivery of antimicrobial proteins. In practise, there are likely to be many more suitable candidate protein drugs, since lysozyme is only active against specific bacterial strains [41]. For example, patches loaded with the antifungal peptide histatin-5 may be effective against chlorhexidine resistant periodontal *Candida* biofilms [43]. The food-grade preservative nisin has broad spectrum activity against many Gram-positive bacteria, and could potentially be incorporated into the patches to treat multi-species bacterial biofilms [44]. The patch technology reported here holds great promise as a novel therapeutic protein delivery system for the oral mucosa.

## CRediT authorship contribution statement

**Jake G. Edmans:** Conceptualization, Methodology, Investigation, Visualization, Writing - original draft. **Craig Murdoch:** Conceptualization, Methodology, Writing - review & editing, Supervision. **Martin E. Santocildes-Romero:** Conceptualization, Supervision. **Paul V. Hatton:** Conceptualization, Writing - review & editing, Supervision. **Helen E. Colley:** Conceptualization, Writing - review & editing, Supervision, Funding acquisition. **Sebastian G. Spain:** Conceptualization, Methodology, Writing - review & editing, Supervision, Funding acquisition.

## Declaration of competing interest

The authors declare the following financial interests/personal relationships which may be considered as potential competing interests: The research presented was funding in part by AFYX Therapeutics. Dr H, Mr J Edmans, Dr S Spain and Professor C Murdoch declare that they have no other known competing financial interests or personal relationships that could have appeared to influence the work reported within this paper.

Dr M E. Santocildes-Romero is employed by AFYX Therapeutics. Professor P V. Hatton is on the AFYX Therapeutics APS Scientific Advisory Board, where AFYX have translated mucoadhesive electrospun patch technology for clinical use and have intellectual property (international patent application WO 2017/085262 A).

## Acknowledgements

The authors would like to thank Jason Heath for training in microbiology, Katharina Clitherow for training and advice in electrospun materials. This work was funded by the UK EPSRC (EP/L016281/1) as a CASE PhD studentship with the Centre for Doctoral Training in Polymers & Soft Matter where AFYX Therapeutics was the industrial partner.

## Appendix A. Supplementary data

Supplementary data to this article can be found online at https://doi.org/10.1016/j.msec.2020.110917.

## References

[1] F. Albericio, H.G. Kruger, Therapeutic peptides, Future Med. Chem. 4 (2012) 1527–1531, https://doi.org/10.4155/fmc.12.94.
[2] J.L. Lau, M.K. Dunn, Therapeutic peptides: historical perspectives, current development trends, and future directions, Bioorg. Med. Chem. 26 (2018) 2700–2707, https://doi.org/10.1016/j.bmc.2017.06.052.
[3] H. Altman, D. Steinberg, Y. Porat, A. Mor, D. Fridman, M. Friedman, G. Bachrach, In vitro assessment of antimicrobial peptides as potential agents against several oral bacteria, J. Antimicrob. Chemother. 58 (2006) 198–201, https://doi.org/10.1093/jac/dkl181.
[4] K. Kavanagh, S. Dowd, Histatins: antimicrobial peptides with therapeutic potential, J. Pharm. Pharmacol. 56 (2004) 285–289, https://doi.org/10.1211/0022357022971.
[5] K. Fujisawa, Y. Miyamoto, M. Nagayama, Basic fibroblast growth factor and epidermal growth factor reverse impaired ulcer healing of the rabbit oral mucosa, J. Oral Pathol. Med. 32 (2003) 358–366, https://doi.org/10.1034/j.1600-0714.2003.t01-1-00111.x.
[6] J.P. Hong, S.W. Lee, S.Y. Song, S.D. Ahn, S.S. Shin, E.K. Choi, J.H. Kim, Recombinant human epidermal growth factor treatment of radiation-induced severe oral mucositis in patients with head and neck malignancies, Eur. J. Cancer Care (Engl.) 18 (2009) 636–641, https://doi.org/10.1111/j.1365-2354.2008.00971.x.
[7] A. Verma, N. Kumar, R. Malviya, P.K. Sharma, Emerging trends in noninvasive

insulin delivery, J. Pharm. 2014 (2014) 1–9, https://doi.org/10.1155/2014/378048.
[8] Z. C., R.J. M., Buccal transmucosal delivery of calcitonin in rabbits using thin-film composites, Pharm. Res. 19 (2002) 1901–1906, https://doi.org/10.1023/102146201.
[9] J. Autio-Gold, The role of chlorhexidine in caries prevention, Oper. Dent. 33 (2008) 710–716, https://doi.org/10.2341/08-3.
[10] M. Innocenti, G. Moscatelli, S. Lopez, Efficacy of Gelclair in reducing pain in palliative care patients with oral lesions, J. Pain Symptom Manag. 24 (2002) 456–457, https://doi.org/10.1016/S0885-3924(02)00524-9.
[11] R.J. Bensadoun, J. Daoud, B. El Gueddari, L. Bastit, R. Gourmet, A. Rosikon, C. Allavena, P. Céruse, G. Calais, P. Attali, Comparison of the efficacy and safety of miconazole 50-mg mucoadhesive buccal tablets with miconazole 500-mg gel in the treatment of oropharyngeal candidiasis: a prospective, randomized, single-blind, multicenter, comparative, phase III trial in patients, Cancer 112 (2008) 204–211, https://doi.org/10.1002/cncr.23152.
[12] V. Hearnden, V. Sankar, K. Hull, D. Vidovi, M. Greenberg, A.R. Kerr, P.B. Lockhart, L.L. Patton, S. Porter, M.H. Thornhill, New developments and opportunities in oral mucosal drug delivery for local and systemic disease, Adv. Drug Deliv. Rev. 64 (2012) 16–28, https://doi.org/10.1016/j.addr.2011.02.008.
[13] N.L. Schechter, S.J. Weisman, M. Rosenblum, B. Bernstein, P.L. Conard, The use of oral transmucosal fentanyl citrate for painful procedures in children, Pediatrics 95 (1995) 335 LP–339 http://pediatrics.aappublications.org/content/95/3/335.abstract.
[14] M.E. Santocildes-Romero, L. Hadley, K.H. Clitherow, J. Hansen, C. Murdoch, H.E. Colley, M.H. Thornhill, P.V. Hatton, Fabrication of electrospun mucoadhesive membranes for therapeutic applications in oral medicine, ACS Appl. Mater. Interfaces 9 (2017) 11557–11567, https://doi.org/10.1021/acsami.7b02337.
[15] H.E. Colley, Z. Said, M.E. Santocildes-Romero, S.R. Baker, K. D'Apice, J. Hansen, L.S. Madsen, M.H. Thornhill, P.V. Hatton, C. Murdoch, Pre-clinical evaluation of novel mucoadhesive bilayer patches for local delivery of clobetasol-17-propionate to the oral mucosa, Biomaterials. 178 (2018) 134–146, https://doi.org/10.1016/j.biomaterials.2018.06.009.
[16] K.H. Clitherow, C. Murdoch, S.G. Spain, A.M. Handler, H.E. Colley, M.B. Stie, H. Mørck Nielsen, C. Janfelt, P.V. Hatton, J. Jacobsen, Mucoadhesive electrospun patch delivery of lidocaine to the oral mucosa and investigation of spatial distribution in a tissue using MALDI-mass spectrometry imaging, Mol. Pharm. 16 (2019) 3948–3956, https://doi.org/10.1021/acs.molpharmaceut.9b00535.
[17] D.B. Khadka, D.T. Haynie, Protein- and peptide-based electrospun nanofibers in medical biomaterials, Nanomed. Nanotechnol. Biol. Med. 8 (2012) 1242–1262, https://doi.org/10.1016/j.nano.2012.02.013.
[18] V. Beachley, X. Wen, Polymer nanofibrous structures: fabrication, biofunctionalization, and cell interactions, Prog. Polym. Sci. 35 (2010) 868–892, https://doi.org/10.1016/j.progpolymsci.2010.03.003.
[19] S.Y. Chew, J. Wen, E.K.F. Yim, K.W. Leong, Sustained release of proteins from electrospun biodegradable fibers, Biomacromolecules 6 (2005) 2017–2024, https://doi.org/10.1021/bm0501149.
[20] K. Wei, Y. Li, X. Lei, H. Yang, A. Teramoto, J. Yao, K. Abe, F.K. Ko, Emulsion electrospinning of a collagen-like protein/PLGA fibrous scaffold: empirical modeling and preliminary release assessment of encapsulated protein, Macromol. Biosci. 11 (2011) 1526–1536, https://doi.org/10.1002/mabi.201100141.
[21] H. Qu, S. Wei, Z. Guo, Coaxial electrospun nanostructures and their applications, J. Mater. Chem. A 1 (2013) 11513–11528, https://doi.org/10.1039/c3ta12390a.
[22] H. Jiang, Y. Hu, Y. Li, P. Zhao, K. Zhu, W. Chen, A facile technique to prepare biodegradable coaxial electrospun nanofibers for controlled release of bioactive agents, J. Control. Release 108 (2005) 237–243, https://doi.org/10.1016/j.jconrel.2005.08.006.
[23] W. Ji, F. Yang, J.J.J.P. Van Den Beucken, Z. Bian, M. Fan, Z. Chen, J.A. Jansen, Fibrous scaffolds loaded with protein prepared by blend or coaxial electrospinning, Acta Biomater. 6 (2010) 4199–4207, https://doi.org/10.1016/j.actbio.2010.05.025.
[24] J. Schindelin, I. Arganda-carreras, E. Frise, V. Kaynig, T. Pietzsch, S. Preibisch, C. Rueden, S. Saalfeld, B. Schmid, J. Tinevez, D.J. White, V. Hartenstein, P. Tomancak, A. Cardona, PBMCs, Nat. Methods 9 (2012) 676–682, https://doi.org/10.1038/nmeth.2019.Fiji.
[25] D. Shugar, The measurement of lysozyme activity and the ultra-violet inactivation of lysozyme, Biomed. Biochim. Acta 8 (1952) 302–309, https://doi.org/10.1016/0006-3002(52)90045-0.
[26] M.E. Aulton, M. Banks, I.I. Davies, A fluorescent technique for the observation of polyvinylpyrrolidone binder distribution in granules, Drug Dev. Ind. Pharm. 4 (1978) 537–539, https://doi.org/10.3109/03639047809081825.
[27] P.B. Jeppesen, B. Hartmann, J. Thulesen, J. Graff, J. Lohmann, B.S. Hansen, F. Tofteng, S.S. Poulsen, J.L. Madsen, J.J. Holst, P.B. Mortensen, Glucagon-like peptide 2 improves nutrient absorption and nutritional status in short-bowel patients with no colon, Gastroenterology 120 (2001) 806–815, https://doi.org/10.1053/gast.2001.22555.
[28] C.H. Chesnut, M. Azria, S. Silverman, M. Engelhardt, M. Olson, L. Mindeholm, Salmon calcitonin: a review of current and future therapeutic indications, Osteoporos. Int. 19 (2008) 479–491, https://doi.org/10.1007/s00198-007-0490-1.
[29] R.M. Neer, C.D. Arnaud, J.R. Zanchetta, R. Prince, G.A. Gaich, J.-Y. Reginster, A.B. Hodsman, E.F. Eriksen, S. Ish-Shalom, H.K. Genant, O. Wang, D. Mellström, E.S. Oefjord, E. Marcinowska-Suchowierska, J. Salmi, H. Mulder, J. Halse, A.Z. Sawicki, B.H. Mitlak, Effect of parathyroid hormone (1-34) on fractures and bone mineral density in postmenopausal women with osteoporosis, N. Engl. J. Med. 344 (2001) 1434–1441, https://doi.org/10.1056/NEJM200105103441904.
[30] R. Giordano, A. Salleo, S. Salleo, F. Wanderlingh, Viscosity and density of lysozyme in water, Phys. Lett. A 70 (1979) 64–66, https://doi.org/10.1016/0375-9601(79)90329-3.
[31] T.T. Herskovits, H. Jaillet, Structural stability and solvent denaturation of myoglobin, Science (80-.) 163 (1969) 282–285, https://doi.org/10.1126/science.163.3864.282.
[32] Y.R. Personna, L. Slater, D. Ntarlagiannis, D. Werkema, Z. Szabo, Electrical signatures of ethanol-liquid mixtures: implications for monitoring biofuels migration in the subsurface, J. Contam. Hydrol. 144 (2013) 99–107, https://doi.org/10.1016/j.jconhyd.2012.10.011.
[33] M. Guettari, A. Belaidi, T. Tajouri, Polyvinylpyrrolidone behavior in water/ethanol mixed solvents: comparison of modeling predictions with experimental results, J. Solut. Chem. 46 (2017) 1404–1417, https://doi.org/10.1007/s10953-017-0649-0.
[34] N. Bhardwaj, S.C. Kundu, Electrospinning: a fascinating fiber fabrication technique, Biotechnol. Adv. 28 (2010) 325–347, https://doi.org/10.1016/j.biotechadv.2010.01.004.
[35] K. Nartetamrongsutt, G.G. Chase, The influence of salt and solvent concentrations on electrospun polyvinylpyrrolidone fiber diameters and bead formation, Polymer (Guildf) 54 (2013) 2166–2173, https://doi.org/10.1016/j.polymer.2013.02.028.
[36] J. Xie, C.H. Wang, Electrospun micro- and nanofibers for sustained delivery of paclitaxel to treat C6 glioma in vitro, Pharm. Res. 23 (2006) 1817–1826, https://doi.org/10.1007/s11095-006-9036-z.
[37] T.H.B. Eriksen, E. Skovsen, P. Fojan, Release of antimicrobial peptides from electrospun nanofibres as a drug delivery system, J. Biomed. Nanotechnol. 9 (2013) 492–498, https://doi.org/10.1166/jbn.2013.1553.
[38] S.-F. Chou, D. Carson, K.A. Woodrow, Current strategies for sustaining drug release from electrospun nanofibers, J. Control. Release 220 (2015) 584–591, https://doi.org/10.1016/j.jconrel.2015.09.008.
[39] F.E. Dewhirst, T. Chen, J. Izard, B.J. Paster, A.C.R. Tanner, W.H. Yu, A. Lakshmanan, W.G. Wade, The human oral microbiome, J. Bacteriol. 192 (2010) 5002–5017, https://doi.org/10.1128/JB.00542-10.
[40] K.Y. Lee, M.R. Jeong, S.M. Choi, S.S. Na, J.D. Cha, Synergistic effect of fucoidan with antibiotics against oral pathogenic bacteria, Arch. Oral Biol. 58 (2013) 482–492, https://doi.org/10.1016/j.archoralbio.2012.11.002.
[41] V.J. Iacono, B.J. MacKay, S. DiRienzo, J.J. Pollock, Selective antibacterial properties of lysozyme for oral microorganisms, Infect. Immun. 29 (1980) 623–632.
[42] J.R.L. Walker, A.C. Hulme, The inhibition of the phenolase from apple peel by polyvinylpyrrolidone, Phytochemistry 4 (1965) 677–685.
[43] C.R. Pusateri, E.A. Monaco, M. Edgerton, Sensitivity of Candida albicans biofilm cells grown on denture acrylic to antifungal proteins and chlorhexidine, Arch. Oral Biol. 54 (2009) 588–594, https://doi.org/10.1016/j.archoralbio.2009.01.016.
[44] J.M. Shin, I. Ateia, J.R. Paulus, H. Liu, J.C. Fenno, A.H. Rickard, Y.L. Kapila, Antimicrobial nisin acts against saliva derived multi-species biofilms without cytotoxicity to human oral cells, Front. Microbiol. 6 (2015) 1–14, https://doi.org/10.3389/fmicb.2015.00617.